On the Impact of Tactical Track Loading on Volume Revisit Performance and the Role of Augmenting Hosted Payloads – A GEO Space Domain Awareness Challenge

Jeffrey Asher, Douglas Cool, Diego Cavero, Joshua Sloane, Kelly Brinkley
JHU Applied Physics Laboratory
Anthony Rosati, Hillary Keltner
Capt., United States Air Force, USSF/SMC/SPGZ

ABSTRACT

Space-based optical sensors have been leveraged previously for timely revisit of geosynchronous orbit (GEO) and tracking of GEO resident space objects. As a result, some electro-optical sensors have been designed to be capable of both object-based tasking to perform tactical track, and volume-based tasking to perform rapid volume revisit. Although some sensor systems are capable of meeting search requirements and track requirements independently, it is unclear how search capability decreases as sensors are tasked to track more objects. In order to preserve timely search capability during periods of high track need, the United States Space Force (USSF) is interested in the ability of low cost, hostable search sensors for GEO space domain awareness (SDA).

This effort leverages Johns Hopkins University Applied Physics Laboratory's (JHUAPL) Chimera tool to investigate the relationship between volume revisit capability and tactical track loading for a notional space-based architecture of optical sensors. Volume revisit performance is presented as the interval between successive collections of a given volume element for a variety of track loads. Results show that volume revisit performance decreases non-linearly with increasing track loading. This decrease in performance is notable specifically in the local noon region where sensor access is thin. The results suggest that the baseline architecture, when augmented with a constellation of hosted search sensors is capable of maintaining adequate revisit performance even in times of high track demand.

1. DISTRIBUTION STATEMENT

2. INTRODUCTION

Space Domain Awareness is composed of multiple functional areas to provide a variety of information regarding known space objects, discovery of new objects, and the overall space environment [1]. To meet the needs of these functional areas, the United States Space Surveillance Network (SSN) is primarily composed of ground-based optical sensors, ground-based radars, and space-based optical sensors. As the proliferation of space technology continues and commercial operations in GEO mature, the importance of persistent SDA is paramount for enforcing norms of behavior and responsible space operations. Space-based optical sensors in GEO are an option to enable this persistence and close the existing solar outages present with the current ground-and-LEO-based architecture. Space telescopes are often required to be capable of search-based and object-based tasking. These sensors are capable of meeting required metrics for both tasks individually, but it is unclear how performance varies when systems are asked to perform both functions simultaneously.

Previous studies have investigated the relative value of 100% search-based vs 100% object-based tasking [3, 4]. To our knowledge, no model has been put forth to investigate the expected performance of an arbitrary mix of search-based and object-based tasking for a heterogeneous sensor architecture. As a result, JHU/APL, in support of the USSF's Space and Missile Systems Center Space Domain Awareness Division Space-Based Electro-Optical Branch (SMC/SPGZ), has developed a tool for assessing volume revisit and tactical track capacity in conjunction, named Chimera. The chimera, as described in Greek mythological, is a creature depicted as a lion with the head of a goat

protruding from its back. The lion, as an apex predator, has eyes specially attuned for tracking, while the goat has eyes designed for searching for predators. The chimera is the namesake for this tool as it encompasses the benefits of both the lion (track) and the goat (search) in one.

Fig. 1: Chimera tool logo.

The JHU/APL Chimera tool provides a geometric assessment of sensor access vs GEO longitude and local time of day, in order to better quantify the benefits of low cost augmenting sensors, commercial hosted payloads, and sensors from proposed international partnerships. Chimera is currently being used to inform ongoing SDA architecture design trades and assess individual sensor contributions to the overall GEO SDA architecture.

Hosted payloads offer a potential affordable solution to perform surveillence of the GEO belt. This paper analyzes the impact of track loading on volume revisit performance for multiple architectures. These architectures highlight the benefits of a notional hosted payload constellation to provide SDA information. The following sections provide more detail into the methodology and assumptions inherent to the current version of the Chimera tool, discuss the simulation setup and primary cases of interest, summarize the results, and mark the key conclusions.

3. METHODOLOGY

Chimera Model 1.0 evaluates the performance of a constellation of geostationary sensors conducting volume revisit observations of the GEO belt. Since all sensors are geostationary, their position is defined simply by their longitude in the GEO belt. A sensor observes a region of the GEO belt between a minimum and maximum standoff longitude distance from it. The sensor has a rectangular field-of-view azimuth/elevation. The operating times are the times when the sensor is looking East or West. A sensor can have overlapping times, when it is looking in both directions. The unloaded volume revisit rate $t_{VR,u}$ is the time for the sensor to scan its observation region when looking in one direction, and with no tactical track loading. Finally, the track load is the percent of time the sensor spends doing tactical track when looking in one direction.

The inputs to the model are the sensor settings defined above for each sensor in the constellation. A Matlab driver tool loads the inputs, creates the scan pattern for each sensor, sets up, and runs an STK scenario. In STK, the sensors execute their scan pattern. STK generates an access report, which says when each sensor has access to each grid point on a longitude band around the GEO belt. This access report is loaded into Matlab for post-processing and analysis.

3.1 Scan Pattern

A sensor's observation region is defined based on the minimum and maximum standoff longitude distance from the sensor, as well as the maximum latitude of the GEO belt to be observed. When converted to the sensor's azimuth/elevation frame, this is a non-rectangular region, as seen in Fig. 2. The scan pattern is generated to encapsulate the observation region.

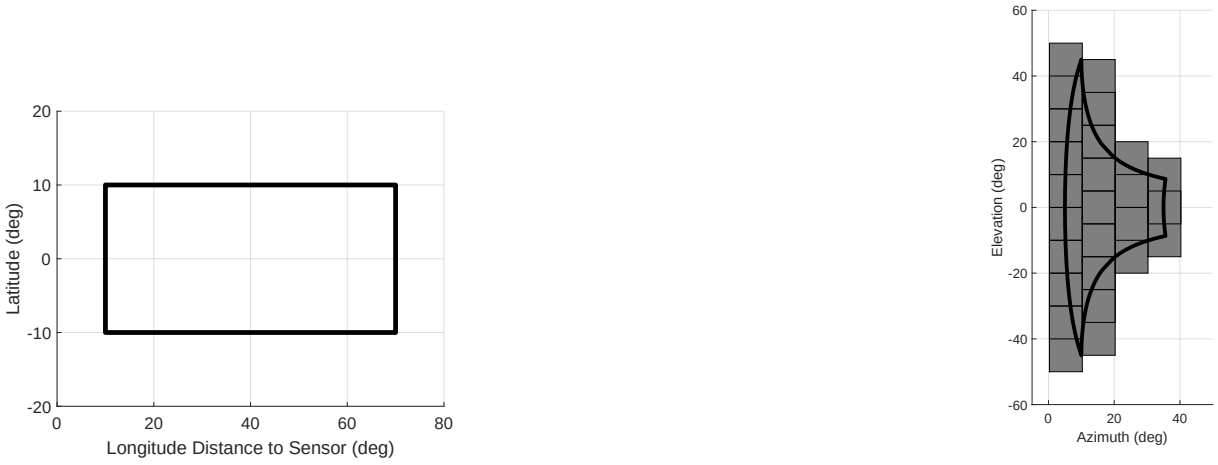

(a) (b)

Fig. 2: A sensor observes a rectangular region of space, such as Fig. 2a. This corresponds to the thick line in Fig. 2b. Each box corresponds to a frame in the scan pattern based on the sensor's field-of-view.

Fig. 2b highlights some tradeoffs which must be made when defining a sensor's operating region. Shorter longitude distances to the sensor require more frames to cover an equivilant region in latitude/longitude space when looking further away, especially at the higher latitudes. However, the minimum detectible object (MDO) size at further distances is larger, or requires a longer integration time to achieve the same MDO size. Finally, the solar phase angle may be worse at further distances for critical parts of the day.

3.2 Track Loading

A dual-use sensor alternates between conducting tactical track (TT) observations of known objects, and volume revisit (VR) of the GEO belt with the goal of discovery of unknown objects. For this paper, we assume that tactical track will be priority. In addition, TT and VR observations are assumed to be independent, with no serruptitious observations. As the tactical track demand increases, the time for the sensor to complete volume revisit increases, while the volume being observed is not changed.

Consider a sensor with a 30s collection time per frame t_{coll}. With no TT load, the volume revisit time is 15 min. Now, consider there are n_{req} known objects requiring TT. The sensor's capacity N_{cap} is the maximum number of objects that can be tracked (i.e. with 100% TT load).

$$N_{cap} = \frac{t_{req}}{t_{coll}} \tag{1}$$

The tactical track load fraction f_{TT} is the fraction of time that the sensor spends doing TT observations.

$$f_{TT} = \frac{n_{req}}{N_{cap}} \tag{2}$$

As n_{req} increases, the number of frames in the scan pattern stays the same. The VR scan will pause every t_{req} minutes to perform TT, in order to meet the required TT cadence. This stretches out the total time to complete the VR scan t_{VR} from the unloaded time $t_{VR,u}$, as shown in Fig. 3.

$$t_{VR} = \frac{t_{VR,u}}{1 - f_{TT}} \tag{3}$$

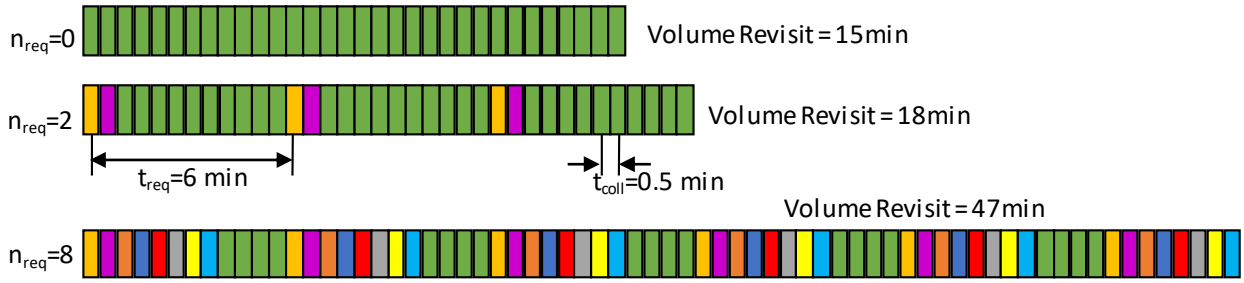

Fig. 3: Effect of tactical track load on volume revisit scan time

When the sensor is looking both ways, the region of space is doubled, and therefore the scan time is doubled. In addition, we assume that the number of TT objects doubles, while t_{req} stays the same, therefore the required tactical track load is doubled. Let δ equal 1 when the sensor is looking one way, and 2 when the sensor is looking both East and West. The total volume revisit time, accounting for the possibilty of looking both ways, is

$$t_{VR} = \frac{t_{VR,u}\ \delta}{1 - (f_{TT}\ \delta)} \tag{4}$$

As expected, as the tactical track load goes to 100%, the volume revisit cadence goes to infinity. This also limits f_{TT} looking one way to 50% for sensors which look both ways.

3.3 Sensitivity

The solar phase angle Φ is the angle between the vector frome the sun to the target object and the vector from the target to the sensor. The phase function relates the reflectance of an object. For most objects, such as satellites, the phase function is a complex combination of Lambertian and specular reflection [5, 2]. The specular phase function is constant, and the Lambertian phase function is

$$F(\Phi) = \frac{2}{3\pi^2} + (\pi - \Phi)\, cos(\Phi) \tag{5}$$

with Φ in radians. In this paper, the target objects are modeled as Lambertian spheres. This underestimates reflectances at larger phase angles. With this assumption, the reflected solar irradiance I from the target at the sensor is related to the phase function $F(\Phi)$, the object's diameter d, the object's albedo α, and the range from the sensor to the target r.

$$I \propto F(\Phi)\alpha d^2 r^2 \tag{6}$$

To model sensitivity, we assume that the sensor has a constant minimum detectible irradiance I_0. In this paper, all objects have equal albedo. The minimum detectible object MDO diameter d is the object diameter with irradiance at the sensor fo I_0 for a given range and solar phase angle. The sensor's sesitivity is defiend by a reference MDO d_0 at range r_0 and zero solar phase angle. The MDO diameter d is therefore

$$d = d_0 \sqrt{\frac{\pi}{sin(\Phi) + (\pi - \Phi)\cos(\Phi)}} \tag{7}$$

An example plot for MDO is shown in Fig. 4. This sensor has a reference MDO with diameter d_0 at 70 deg, and 10-70 deg longitude field-of-regard, looking East. In addition to solar exclusion angle constraints, this figure motivates the selected operating period of 10 am - midnight. The sensor can see an object twice the diameter of the reference object at almost any position while the sensor is on.

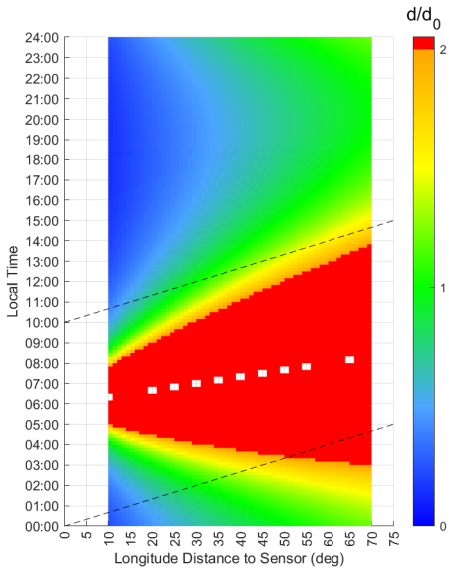

Fig. 4: Minimum detectible object (MDO) diameter d. Sensor with reference MDO with diameter d_0 at 70 deg, and 10-70 deg longitude field-of-regard. Black dotted lines are the sensor's on/off times. This line is at a diagonal because of the conversion between sensor local time to UTC, and back to local time of the observed volume element.

4. RESULTS

4.1 Sensor Architecture

For the purpose of this study, several notional sensors have been defined. The sensor properties are listed in Table 1.

	Sensor	Unloaded Revisit Rate [min]	Max Longitudinal Range [°]	Operating Times [Local] East	Operating Times [Local] West	Track Loading
	Dual-Use East-West Sensor	30	80	1000 - 2400	0000 - 1400	0-100%
30° HP	East Volume Scanning HP	30	40	1000 - 0200	N/A	0%
30° HP	West Volume Scanning HP	30	40	N/A	2200 - 1400	0%
60° HP	East Volume Scanning HP	60	70	1000-0200	N/A	0%
60° HP	West Volume Scanning HP	60	70	N/A	2200 - 1400	0%

Table 1: Sensor properties

For all of these sensors, the minimum longitude range is 10°. At shorter longitudinal distances than this, a large number of scan frames would be needed to cover a relatively small longitude span. In addition, if the sensor's maximum elevation is limited, it would not be able to see the full latitude of interest in this region.

The dual-use East-West sensor represents a high-quality exquisite sensor. It is capable of looking both East and West, and can do a combination of tactical track and volume revisit. In contrast, the hosted payload (HP) sensor represents a low-cost sensor with less capabilities, intended for volume revisit only, and could be flown as a hosted payload. When the HP's maximum range is doubled, its revisit rate is doubled as well. This is only a rough approximation, as it does not account for decrease in number of frames needed to cover the same longitude region when looking further away. It also does not account for the increased integration time required for further ranges, or the decreased sensitivity.

Three architectures were evaluated using these sensors, designed for global coverage of the GEO belt. In the baseline architecture, six East-West sensors are placed uniformly along the GEO belt. This architecture has coverage gaps near

the sensors at noon, due to the sensor minimum longitude range and operating time. In the second architecture, HPs with 30° longtiude coverage are added to augment the baseline. This includes 12 East facing HPs and 12 West facing HPs, placed to cover the noon gaps of the East-West sensors. The final architecture is similar, now half as many HPs, and correspondigly increased revisit rates. The sensor laydowns for each architecture are shown in Fig. 5.

4.2 Analysis

Each architecture was run in Chimea Model 1.0, at various tactical track loads for the East-West sensor. The access report from this model lists the times that each point along the GEO belt is observed by one of the sensors. The revisit interval is the time between two observations. Coordination between multiple sensors observing the same point in space was not optimized for, so in some cases there can be multiple observations back-to-back, leading to alternating interval times. Fig. 5 shows plots of the interval times vs. longitude on the GEO belt, and local time of day for the longitude.

At 0% TT, the baseline case has good performance, but does have noon gaps near the sensors. As the load increases, the performance decreases. Recall that the TT load is doubled when the sensor is looking in both directions (10 am - 2 pm local). This leads to poor performance during daytime. Space sensors are most needed for SDA during the day, when ground telescopes are not able to make observations. This highlights the challenge with relying on dual-use sensors for both TT and VR.

The architectures augmented by HP sensors attempt to remediate this challenge. In the Baseline + 30° HP architecture, the volume revisit performance at maximum TT load is better than the baseline by iteslf at zero load. This displays the capability of HP sensors to provide a backstop for the baseline architecture when it is tasked heavily to perform TT. At low TT loads, the Baseline + 60° HP architecture has no noon gaps. By 50% TT load, the HPs still provide modest performance with some noon gaps. At 50% loading, this architecture performs comparably to the Baseline case with only 25% loading.

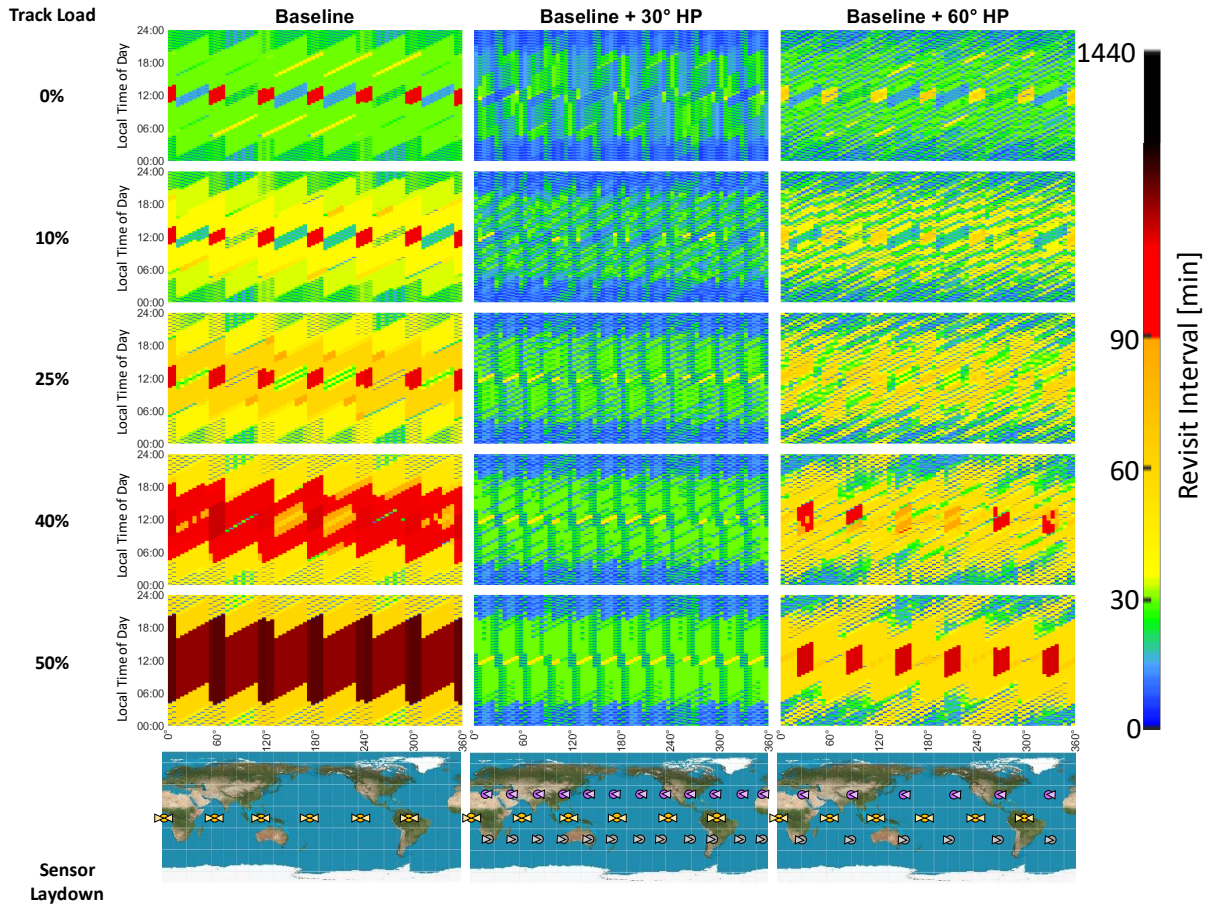

Fig. 5: Comparison of volume revisit capability as a function of Dual-Use East-West Sensor track loading for Left: Baseline, Middle: Baseline + 30° HP augmentation, Right: Baseline + 60° HP Augmentation. Color represents time interval between successive observations.

The figures in Fig. 5 are organized by a mesh grid of points spanning GEO longitude, and local time. The time since last observation (not shown) is the time since the previous observation at a given longitude, for a point. The fraction of points where the time since last observation is greater than 30 minutes is shown in Fig. 6. This corresponds to the spacial and temporal degradations in volume revisit performance as a function of track loading. This fraction display a linear relationship for these architectures.

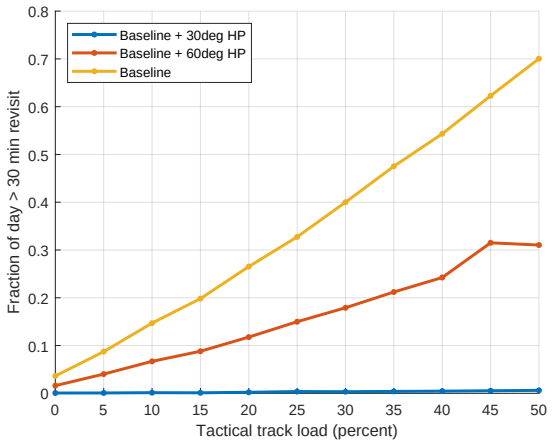

Fig. 6: Fraction of day that has exceeded 30 minute revisit.

Fig. 6 displays a linear relationship with increased track load. The inclusion of hosted payload sensors reduce the overall slope, displaying a preservation in search capability. Table 2 displays linear fit parameters for the data presented in Fig. 6.

Case	Slope	RMS Error	Correlation
Baseline	1.33E-02	4.61E-02	0.979
Baseline + 30° HP	1.14E-04	1.26E-03	0.998
Baseline + 60° HP	6.19E-03	4.20E-02	0.992

Table 2: Linear regression parameters associated with fit to Fig.6 data

For a point on the longitude/time mesh, the interval time is the time between the previous and next observation of the longitude point. Note that this approach applies a uniform mesh. If collections occur with less frequency than the mesh's temporal resolution, multiple mesh points between the collection times will store the same interval time. The average and median value of the interval on the uniform mesh are calculated, and plotted in Fig. 7. Due to the note above, this approach results in a time-weighted avarage and median revisit interval.

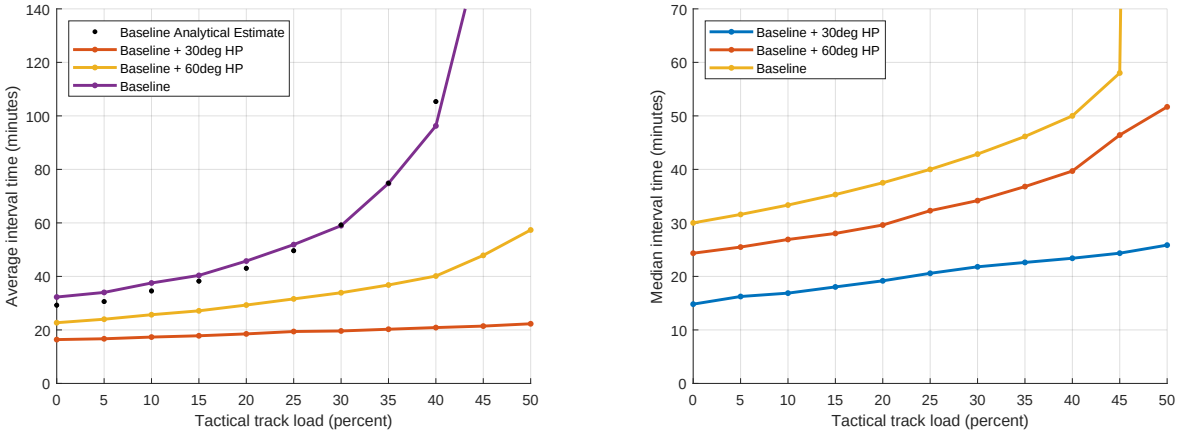

(a) Average

(b) Median

Fig. 7: Revisit interval as a function of tactical track loading.

As seen in Fig. 7a, the time-weighted average interval increases exponentially with load. The addition of hosted payloads to the baseline help to flatten this curve and preserve volume revisit performance. The baseline curve fits an analytical estimate derived from a weighted average of expected revisit times with different asynchronous intervals.

Fig.7 displays the median interval time with of the same data. This view again helps to display the contributions of the HP sensors. Note the large spike in the baseline case is due to the noon-time outage spanning ¿ 50% of the day.

5. CONCLUSIONS

This effort presents a simplified investigation into volume revisit performance as a function of track loading for a variety of hosted payload augmented space architectures. Although this effort is limited in scope to specific, notional sensor architectures, the approach and methodology allows for a flexible framework for rapidly assessing sensor contributions for GEO SDA. Metrics from the Chimera tool show significant impacts to the volume revisit performance of dual use sensors under rising track loads. Hosted payload contributions are most prevalent during periods of high track demand in the local noon region. Hosted payloads have the ability to provide resiliency to search-based SDA mission functions. In times of high track demand, HP sensors maintained volume revisit requirements and covered sensor standoff gaps in the noon-time region. The contributions of hosted payload sensors also have an added benefit of providing resilience to any already existing sensor architecture. Moreover, the choice of hosting sensors specifically in GEO allow for a scalable architecture that can prioritize increasing performance spatially or temporally. Desire for increased performance in a region can be achieved with sensors in the region of interest, while desire for all-day coverage can be achieved by combinations of East-facing and West-facing HP's. To improve volume revisit performance it is imperative to keep the track demand on any dual use systems low, or invest in complementary hosted payload sensors.

6. ACKNOWLEDGEMENTS

The authors would like to acknowledge the contributions from Dr. Joseph Comberiate and Nicholas Dutton, as well as the continued support from Mr. Jack Barnett and USSF/SMC/SPGZ program office.

7. DISCLAIMER

The views expressed are those of the author and do not necessarily reflect the official policy or position of the Department of the Air Force, the Department of Defense, or the U.S. government.

8. REFERENCES

[1] Joint Publication 3-14 Space Operations, 2018.

[2] John Africano, Paul Kervin, Doyle Hall, Paul Sydney, John Ross, Tamara Payne, Steve Gregory, Kira Jorgensen, Kandy Jarvis, Tracy Parr-Thumm, Gene Stansbery, and Ed Barker. Understanding photometric phase angle corrections. In *Fourth European Conference on Space Debris*, volume ESA SP-587, Darmstadt, Germany, 2005.

[3] T. Flohrer, T. Schildknecht, R. Musci, and E. Stoveken. Performance estimation for GEO space surveillance, 2005.

[4] Fred Hertwig, John Colombi, Richard Cobb, and Fred Meyer. Search-Based vs. Task-Based Space Surveillance for Ground-Based Telescopes. In *AMOS Conference*, 2019.

[5] J Hostetler and H Cowardin. Experimentally-Derived Phase Function Approximations in Support of the Orbital Debris Program Office. In *First International Orbital Debris Conference*, 2019.